Multi-plectoneme phase of double-stranded DNA under torsion

Marc Emanuel,[1,2] Giovanni Lanzani,[1] and Helmut Schiessel[1]

[1] *Instituut Lorentz voor de theoretische natuurkunde, Universiteit Leiden,P.O. Box 9506, NL-2300 RA Leiden, The Netherlands*

[2] *Institute of Complex Systems II, Forschungszentrum Jülich, Jülich 52425, Germany*

Abstract

We use the worm-like chain model to study supercoiling of DNA under tension and torque. The model reproduces experimental data for a much broader range of forces, salt concentrations and contour lengths than previous approaches. Our theory shows, for the first time, how the behavior of the system is controlled by a multi-plectoneme phase in a wide range of parameters. This phase does not only affect turn-extension curves but also leads to a non-constant torque in the plectonemic phase. Shortcomings from previous models and inconsistencies between experimental data are resolved in our theory without the need of adjustable parameters.

The DNA contained in every cell of all higher organisms is hundred times longer than the cell diameter: to fit inside it has to fold. This is a challenging problem since DNA is a semi-flexible polymer, making it hard to confine it in small spaces. On the other hand, local unfolding of DNA has to be efficient, as it plays a key role in the transcription and replication of the genome. Unfolding is achieved by stretching and twisting the molecule: unraveling how DNA reacts to them is crucial to understand cellular activities.

The relevant mechanical properties of DNA have been studied with single molecule techniques, where individual molecules are stretched and/or twisted under physiological conditions. The stretching and bending elasticity, in the absence of twisting, has been investigated through measurements of the force-extension relation of DNA [1] and theories based on the worm-like chain (WLC) model have successfully explained the experimental results [2] [3]. The WLC model [4] is a coarse-grained approximation where the particular sequence of basepairs (bp) is hidden by treating the DNA as a homogeneous semiflexible polymer.

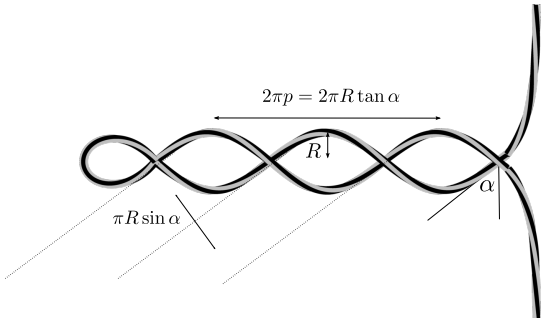

Figure 1. Geometry of the plectoneme.

To understand stretched DNA under torsional stress [5–7] several models based on the WLC framework were proposed. However, they were either purely mechanical [8], involved non-linear elasticity [9], phenomenological [10], aimed only at a certain region of the experimental data [11] or had to invoke a non-canonically reduction of the DNA charge density [12]. The outcome of the experiments still remains poorly understood.

In this Letter we present a theory, based on the WLC model, without any of the aforementioned shortcomings. The results describe experimental data accurately (see Fig. 2 for an example). Up to now it has been assumed that under high twist DNA reduces its torque through the formation of a *single* plectoneme, see Fig. 1. We show here for the first time how thermal fluctuations lead to a *multiple* plectoneme phase instead. We demonstrate its

impact on the turn-extension slope, see Fig. 3, and on the torque, see Fig. 5.

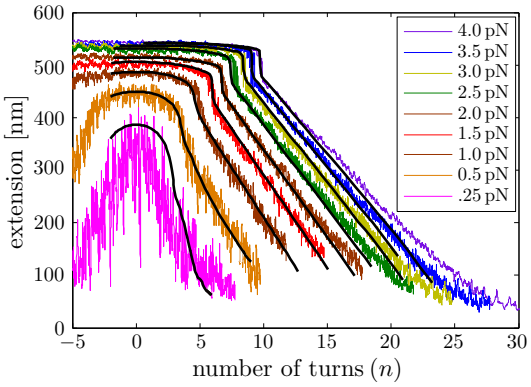

Figure 2. The turn-extension plots of a 600 nm DNA chain at 320 mM ionic strength for various tensions between 0.25 and 4 pN. Comparison between theory and experiments. Experimental data from [12].

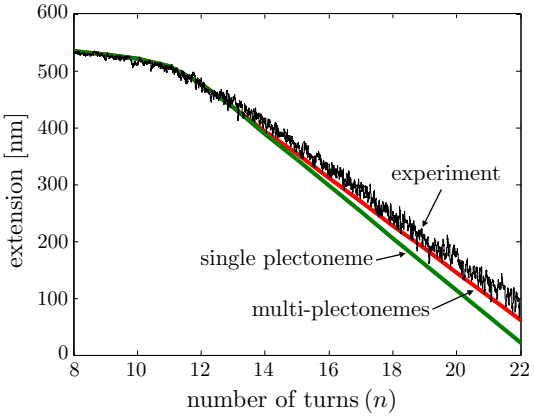

Figure 3. The results of the theory with and without the possibility to form more than one plectoneme are presented alongside the experimental results (3 pN, 20 mM, Experimental data from [12].

In the experiments the DNA is anchored at one end to a surface and at the other end to a magnetic [7] or optical [6] tweezer. This allows to control the tension and the linking number (n), the number of turns inserted, at the same time. Increasing n at constant tension yields turn-extension plots like the ones shown in Fig. 2. Initially most of n goes into twist (Tw) of the molecule while the end-to-end distance remains approximately constant. Then a transition — dependent on the salt concentration, the DNA length and the applied force and often accompanied by a jump [6] — signals the formation of a plectoneme. From this

point onward all the additional n is stored inside the growing plectoneme as writhe (Wr), a quantity related to the path of the polymer. Writhe, twist and linking number are connected through *White's relation* [13], $n = Tw + Wr$.

We assume that the legs and the end loop form a homoclinic solution, characterized by the parameter $t \in [0, 1]$, as described in [14]. $t = 0$ corresponds to a straight rod, and $t = 1$ to the homoclinic loop. Inside the homoclinic solutions, at the point of (non-zero) minimum distance of symmetric points, we insert a plectoneme. Such a minimum exists in the range $0.804 \gtrsim t > 1$; half this distance sets the plectoneme radius $R(t)$. The homoclinic solution stores some fixed amount of writhe, $Wr_l = 2(\arcsin t)/\pi$. Moreover its bending and potential energy sum up to $E_l = 8F\lambda t$. Here F is the tension, $P_b = A/k_BT$ the DNA bending persistence length and $\lambda = \sqrt{A/F}$.

On the other hand, the plectoneme has a bending energy density $e_b = A\cos^4\alpha/2R^2(t)$ and a contribution to the potential energy density of f where α denotes the angle of the plectoneme, Fig. 1. When properly accounting for the presence of the end loop, the plectoneme writhe density is exactly given by $wr_p(t) = \sin\alpha\cos\alpha/2\pi R(t)$. The electrostatic interaction in the plectoneme has a free energy density $f_{\mathrm{el},0}$ described by Ubbink and Odijk [15]. The effective charge density in this contribution is calculated on the basis of a charge density of 2 charges/0.34 nm with the method described in [16].

The zero-temperature energy density of a DNA chain with contour L_c containing m plectonemes of total relative length $l_p \equiv L_p/L_c$ is given by

$$\begin{aligned} e_0(m, l_p) = l_p e_b + m\frac{E_l}{L_c} + l_p(F + f_{\mathrm{el},0}) \\ + 2\pi^2 P_C k_B T(\frac{n}{L_c} - m\frac{Wr_l}{L_c} - l_p wr_p)^2 \end{aligned} \tag{1}$$

where the last term is the twist contribution to the energy, and P_C is the torsional persistence length. However, to properly account for the experimental situation the zero-temperature analysis is not sufficient.

Thermal fluctuations lead to three different contributions: the first affects the DNA legs, the second acts within plectonemes and the last is related to the number of plectonemes and their position and length distribution. Outside the plectonemes, thermal fluctuations modify the shape of the DNA; for a given torque τ they shorten the DNA end-to-end distance by a factor $\rho(F, \tau)$ [17] and give origin to thermal writhe that lowers the twist energy density, which can be expressed as a renormalized torsional persistence length $P_C^{\mathrm{eff}}(\lambda)$ [17].

Inside the plectonemes, following Ref. [15] we consider fluctuations in two directions. We denote by σ_r (σ_p) the standard deviation in the radial (pitch) direction. The fluctuations in the pitch direction are set by the geometry: $\sigma_p = \pi R \sin\alpha$, see Fig. 1, while in the other direction they are set by the electrostatic repulsion. Their contribution changes the electrostatic energy, up to first order, to $f_{\rm el} = f_{\rm el,0} \times \exp(4\kappa^2\sigma_r^2)$ [15], where κ^{-1} is the Debije length. The presence of twist couples the two directions of the fluctuations, an effect not studied before [18]. This result in a new effective deflection length:

$$\bar{\lambda} = 2\frac{\lambda_r^3\lambda_p + \lambda_r^2\lambda_p^2 + \lambda_r\lambda_p^3}{(\lambda_r + \lambda_p)(\lambda_r^2 + \lambda_p^2)} \tag{2}$$

where $\lambda_{r,p} = (P_b\langle\sigma_{r,p}^2\rangle)^{1/3}$ are the deflection lengths of confinement as defined in Ref. [19]. The resulting twist energy density, renormalized with $P_C^{\rm eff}(\bar{\lambda})$, depends on the confinement. Since twist diffusion happens on a very short time scale, the twist energy density in the legs and in the plectonemes should be the same. This non-trivially couples the linking number density between legs and plectonemes.

As a consequence of thermal fluctuations, the plectonemes' path is shortened by $\rho_{\rm str}$, its bending energy density (e_b) and bare writhe density (wr_b) are modified; the confinement of the polymer contributes an additional $f_{\rm conf}$ to the free energy [20]. Together with the change from $f_{\rm el,0}$ to $f_{\rm el}$, these modify $e_0(m, l_p)$ to $f(m, l_p)$.

In the infinite chain limit, as long as the number of plectonemes stays small, the plectoneme parameters R, α and σ_r become independent of l_p since end loop contributions drop out.

The final contribution of the fluctuations comes from two combinatorial factors in the partition function. They arise from the number of ways the total length of the plectonemes can be distributed between them, and the number of ways the plectonemes can be placed along the DNA. Since the quantities involved are continuous we need to impose a ξ-cutoff in our calculations which we assume in the following to be given by the DNA helical repeat, $\xi = 3.4\,\text{nm}$. Assuming hard-core interactions between the plectonemes, this results in the partition function

$$Z = Z_0 + \sum_{m=1} \int \mathrm{d}L_p G(m, L_p) e^{-\beta f(m,l_p)L_c} \tag{3}$$

$$G = \frac{(\rho(L_c - L_p) - mL_{\rm loop})^m}{\xi^m m!} \frac{L_p^{m-1}}{\xi^{m-1}(m-1)!}. \tag{4}$$

Here Z_0 is the partition function when $m = 0$ and $L_{\rm loop}$ is the length of a single end loop. The first factor of G is the number of ways one can arrange m plectonemes along the DNA; the second factor is the number of ways the length L_p can be distributed between m plectonemes.

When $\partial_n m L_{\rm loop} \ll \partial_n L_p$ the system is in the single-plectoneme state. On the other hand, for $\partial_n m L_{\rm loop} \approx \partial_n L_p$ the physics of increasing n cannot be described by the notion of plectoneme length growth alone, but a full multi-plectoneme approach is needed. To characterize these two states we introduce the multi-plectoneme parameter η as the difference between the writhe efficiencies of loops and plectonemes

$$\eta \equiv \frac{E_l}{W r_l} - \frac{f_p}{w r_p} \tag{5}$$

where f_p is the free energy density difference between plectoneme and legs. η is important because it enters exponentially the multi-plectoneme parameter ζ

$$\zeta \equiv e^{-W r_l \eta} \left(\frac{W r_l / L_l}{w r_p} \right)^2 . \tag{6}$$

One can show that $\zeta \ll 1$ corresponds to a single-plectoneme state, whereas $\zeta \approx 1$ signals the multi-plectoneme phase. In the inset of Fig 4, ζ is displayed as a function of salt concentration for different tensions.

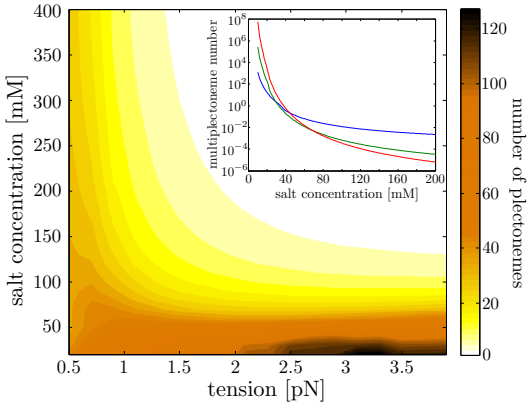

Figure 4. Phase diagram of the average number of plectonemes as a function of tension and salt concentration for a 7.2 μm long chain. Note the shift of the maximum from low tension at high salt to high tension at low salt. The inset shows the multi-plectoneme parameter versus salt concentration for 1 pN (blue), 2 pN (green) and 3 pN (red).

Theories without the possibility of multiple plectonemes, typically predict, for low salt concentrations, a too steep slope of the linear part of the turn-extension curves. As can

be seen in Fig. 3 the multi-plectoneme phase accurately describes the experiments, even for very low salt concentrations (20 mM, data from [12]).

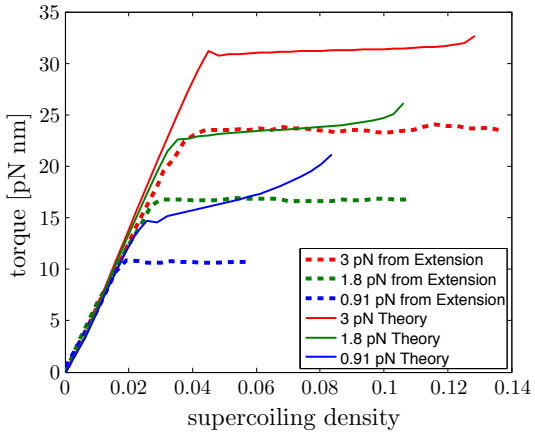

Figure 5. The supercoiling density-torque plots of a 5600 nm DNA chain at 100 mM ionic strength for 0.91 pN, 1.8 pN and 3 pN tension. Comparison between theory and torques inferred from extension measurements. Data taken from [7]

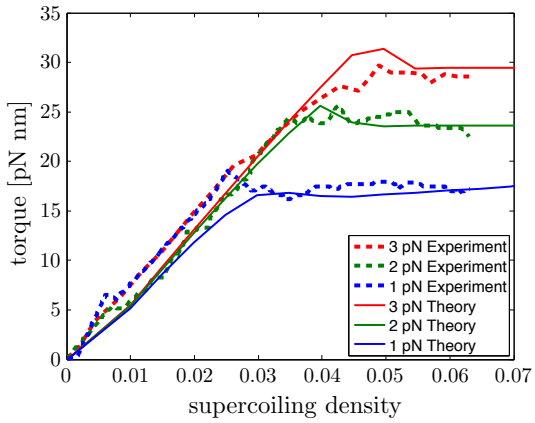

Figure 6. The supercoiling density-torque plots of a 725 nm DNA chain at 100 mM ionic strength for 1 pN, 2 pN and 3 pN tension. Comparison between theory and torques measured using a specially crafted cylinder. Data taken from [6]

Besides the slope, the multi-plectoneme phase influences the torque after the transition. In fact, after the transition into the single-plectoneme phase, n is transferred at a fixed rate into l_p. This results in a small bump in the torque at the transition, caused by the use of a number of turns clamp, followed by a constant plectoneme torque. On the other hand, in the multi-plectoneme phase the entropic contribution to the free energy ceases to

be linear in n. This explains the difference between torques measured in optical tweezer experiments [6] and calculated using Maxwell relations in a magnetic tweezer setup [7]. The latter method is based on the assumption of a constant torque after the transition. However, for the multi-plectoneme phase our theory predicts a non-constant torque. In Fig. 5 we show what our model predicts for the data presented in [7]. To facilitate comparison with the original paper, not the linking number, but the supercoiling density is used, which is defined as the ratio of the linking number density to the linking density of the two strands of free DNA. As can be seen in Fig. 5, the assumption of constant torque underestimates the torque difference between the high and low tension curves. The multi-plectoneme phase prediction, however, correctly reproduces the torque directly measured in [6], as is shown in Fig. 6.

A final consequence of the multi-plectoneme phase is the change in the dynamics of plectonemes in a chain torsionally loaded. Twist mediated plectoneme length redistribution over the plectonemes makes a fast diffusion of plectonemes possible also in the crowded environment of the plasmoid in bacteria or a dense chromatin fiber in eukaryotes. The implications for cellular processes from transcription to segregation are significant.

To conclude: the results of the theory show how the multi-plectoneme phase is crucial to understand the static and dynamic behavior of DNA under tension and torque. The torque in fact is much higher than what was previously computed [7], a fact that could be crucial in the understanding of the life processes in which DNA is involved.

The authors thank Ralf Seidel for providing us with experimental data and Theo Odijk and Ralf Seidel for fruitful discussions. We acknowledge discussions with Cees Dekker and Marijn van Loenhout.

[1] S. B. Smith, L. Finzi, and C. Bustamante, Science **258**, 1122 (1992).

[2] J. F. Marko and E. D. Siggia, Macromolecules **28**, 8759 (1995).

[3] T. Odijk, Macromolecules **28**, 7016 (1995).

[4] M. Doi and S. F. Edwards, *The theory of polymer dynamics* (Oxford University Press, 1988).

[5] T. R. Strick, J.-F. Allemand, D. Bensimon, A. Bensimon, and V. Croquette, Science **271**, 1835 (1996).

[6] S. Forth, C. Deufel, M. Y. Sheinin, B. Daniels, J. P. Sethna, and M. D. Wang, Phys. Rev.

Lett. **100**, 148301 (2008).

[7] F. Mosconi, J. F. Allemand, D. Bensimon, and V. Croquette, Phys. Rev. Lett. **102**, 078301 (2009).

[8] P. K. Purohit, J. Mech. Phys. Solids **56**, 1715 (2008).

[9] M. L. Smith and T. J. Healey, Int. J. Nonlin. Mech. **43**, 1020 (2008).

[10] J. F. Marko, Phys. Rev. E **76**, 021926 (2007).

[11] N. Clauvelin, B. Audoly, and S. Neukirch, Macromolecules **41**, 4479 (2008).

[12] C. Maffeo, R. Schöpflin, H. Brutzer, R. Stehr, A. Aksimentiev, G. Wedemann, and R. Seidel, Phys. Rev. Lett. **105**, 158101 (2010); H. Brutzer, N. Luzzietti, D. Klaue, and R. Seidel, Biophys. J. **98**, 1267 (2010).

[13] G. Călugăreanu, Rev. Roum. Math. Pures Appl. **4** (1959); J. White, Am. J. Math. **91**, 693 (1969).

[14] M. Nizette and A. Goriely, J. Math. Phys. **40**, 2830 (1999).

[15] J. Ubbink and T. Odijk, Biophys. J. **76**, 2502 (1999).

[16] J. Philip and R. A. Wooding, J. Chem. Phys. **113**, 953 (1970).

[17] J. D. Moroz and P. Nelson, Macromolecules **31**, 6333 (1998).

[18] Marc Emanuel, in preparation.

[19] T. Odijk, Macromolecules **16**, 1340 (1983).

[20] M. Emanuel, *Doctoral Thesis*, Ph.D. thesis, Leiden University (2012).